Earth Sciences
2025, Vol. 14, No. 6, pp. 239–260
https://doi.org/10.11648/j.earth.20251406.14

Research Article

Peculiarities of Predicting Synthetic Seismograms and Accelerograms for Heterogeneous Foundation Beddings

Eduard Khachiyan[1, 2, *]

[1]Scientific Departmen, National University of Architecture and Construction of Armenia (NUACA), Yerevan, Armenia
[2]Institute of Geological Sciences, National Academy of Sciences of the Republic of Armenia (NAS RA), Yerevan, Armenia

Abstract

The article offers an improvement of the method for predicting strong ground motion displacements and accelerations, assuming that an earthquake is an instantaneous mechanical rupture of the Earth's crust. The method uses derived theoretical formulas to calculate all three parameters of the ground motion: displacements, velocities and accelerations during strong (with magnitude M≥6.0) earthquakes for any heterogeneous (multilayer) ground beddings. The article addresses the case of heterogeneous two-layer beddings. The example provided involves the results obtained for 16 variants of two-layer heterogeneous sites in seismic categories I-IV at the magnitude M=7.0, and distance of 15 km from the expected earthquake's rupture. A comparison of the results obtained for actual heterogeneous foundation beddings with the equivalent homogeneous beddings showed divergences of increase by 1.3-1.6 times, depending on the number of the five and three natural oscillation modes considered. Significant effects of various modes of foundation bedding natural oscillations on ground surface displacements and accelerations were identified when comparing a heterogeneous beddings to a homogeneous ones. A substantial reduction (by a factor of two or more) in the stiffness of the upper soil layer relative to the lower layer leads to a marked increase in surface ground accelerations. A recommendation is provided that the predicted values of displacements and accelerations for heterogeneous foundation beddings should be calculated with consideration of at least 5 natural oscillation modes of the ground bedding. The paper proposes a new analytical solution to the problem of an earthquake as an instantaneous mechanical rupture of the earth's crust with modified boundary and initial conditions of the problem, and also reveals the influence of the ratio of the rigidities coefficients and the geometric parameters of the layers on the amplitudes of seismograms and accelerograms on the Earth's surface.

Keywords

Heterogeneous Foundation Bedding, Prediction, Synthetic Seismograms and Accelerograms, Seismic Categories of Soils, Higher Mode Oscillations

[*]Corresponding author: edkhach@sci.am (Eduard Khachiyan)

Received: 31 October 2025; **Accepted:** 14 November 2025; **Published:** 19 December 2025

1. Introduction

One of the main issues in seismic resistant construction is the availability of a large number of accelerograms for past earthquakes at the site of a future construction project, recorded during a sufficiently long period. This would allow identifying statistically characteristic types of accelerograms for given site and therefore, reliable designing of the structure through calculations of seismic impact based on the selected accelerogram or a group of accelerograms. However, so far the number of records of past earthquakes in most of the seismically active zones of the Earth has been insufficient due to infrequent occurrences (once in more than 500 years) of strong earthquakes with magnitudes of M≥7.0-8.0 and intensities of I=0.3g-0.8g [1-4]. In addition, the first reliable accelerographs appeared only in 1940s.

Seismic load is inertial and dynamic in nature. Therefore, seismic hazard parameters for a given site primarily depend on the values of horizontal (vertical, rotational) ground motion accelerations and their changes over the time. This proves the importance of studying the issues related to creation of artificial seismograms and accelerograms for strong earthquakes that would have adequate properties of actual recorded earthquakes. A short review of this issue was published in the initial articles [5, 6], where for the general case, foundation bedding was assumed to be heterogeneous, multi-layer (*n*-layer), but without specifying the layer parameters of thickness, density and stiffness. The results of the studies for a large number of single-layer homogeneous foundation beddings were published in the mentioned articles, as well as in [7] by E. Khachyan, and many experts regard them close to the results recorded during actual strong earthquakes. In this study a simple two-layer bedding is considered to make sure the results are illustrative. The choice of heterogeneous two-layer bedding is based on the fact that the ratio of vs1 and v_{s2} propagation velocities of displacement waves in the soil during strong earthquakes significantly influences the ground surface displacement and acceleration values. In many cases, the cause of structural failure is the low shear wave velocity of the first soil layer v_{s1} compared to the underlying layer v_{s2}. Furthermore, any typical multilayered foundation can be effectively represented as a two-layer foundation with equivalent dynamic and seismic properties, according to formulas provided in seismic design codes used in many countries, including Armenia [8]. Therefore, the main objective of this study is to cover a wide range of possible cases (18 cases are analyzed in the article), involving various ratios of v_{s1} to v_{s2} for two-layer foundation beddings and different thicknesses of layers H_1 and H_2. In some cases, to ensure the seismic resistance of a particular structure founded on a multilayer soil profile, it may be advisable to preemptively remove the overly soft upper soil layers.

2. Problem Statement

Below are some of the fundamental assumptions, equations, and parameter relationships of the problem, derived and utilized by E. Khachiyan [5-7]. The near-surface upper soil layers differ significantly in kinematic conditions and physical-mechanical properties from the deeper layers of rock (Figure 1). These upper layers are less dense, with their elasticity coefficients under tension E and shear modulus G up to twice lower than those of the deeper rocks. Moreover, they are subjected to substantially lower vertical compressive stresses, and their volume is small compared to the total volume of the fractured blocks. Due to these characteristics, they exhibit greater shear deformability in both horizontal and vertical directions relative to the deeper layers. Therefore, during an instantaneous rupture of the Earth's crust, the rocks of the upper layers experience much more intense *alternating dynamic displacements, generated by inertial forces of the rock mass*, than the deep layers. During a real earthquake, seismographs and accelerographs record precisely these alternating displacements and accelerations of soil particles on the Earth's surface.

If a near-surface prismatic zone is isolated from the rock mass at a distance Δ from the rupture, having a uniform width and thickness $H<<H_0$, where $H+H_0$ is the depth to the rupture (Figure 1a), this zone at any point along the rupture length L will represent a multilayer lithological column with varying physical-mechanical and geometric properties: densities ρ_k, shear moduli G_k, and thicknesses H_k (Figure 1b). Here, the depth H is defined as the distance from the Earth's surface (from the design level of the structure) to the dense bedrock with shear wave velocities exceeding 1000 m/s, but *not less than 30 meters*. Numerous records of actual earthquakes simultaneously recorded both at the surface and at depths up to 150 meters demonstrate a significant attenuation of seismic effects with depth [9]. This is also evidenced by the low damage observed to underground structures during strong earthquakes [2]. It is well established that *the structure of the near-surface multilayer soil stratum* significantly influences the characteristics of seismic vibrations at Earth's surface.

Based on this, the current study assumes that *during an instantaneous rupture, the effect of inertial displacements of the deeper layers on the inertial displacements of the upper near-surface layers can be neglected* (Figure 1b). Thus, for the design scheme to determine the time history patterns of displacements (seismograms) and accelerations (accelerograms) of soil particles motion at the Earth's surface, the multilayer lithological column of height H (Figure 1b, c, d) is considered. All layers of this column at the initial $t=0$ are assigned initial velocities of $v(M,\Delta)$, according to formula (2) and Table 1.

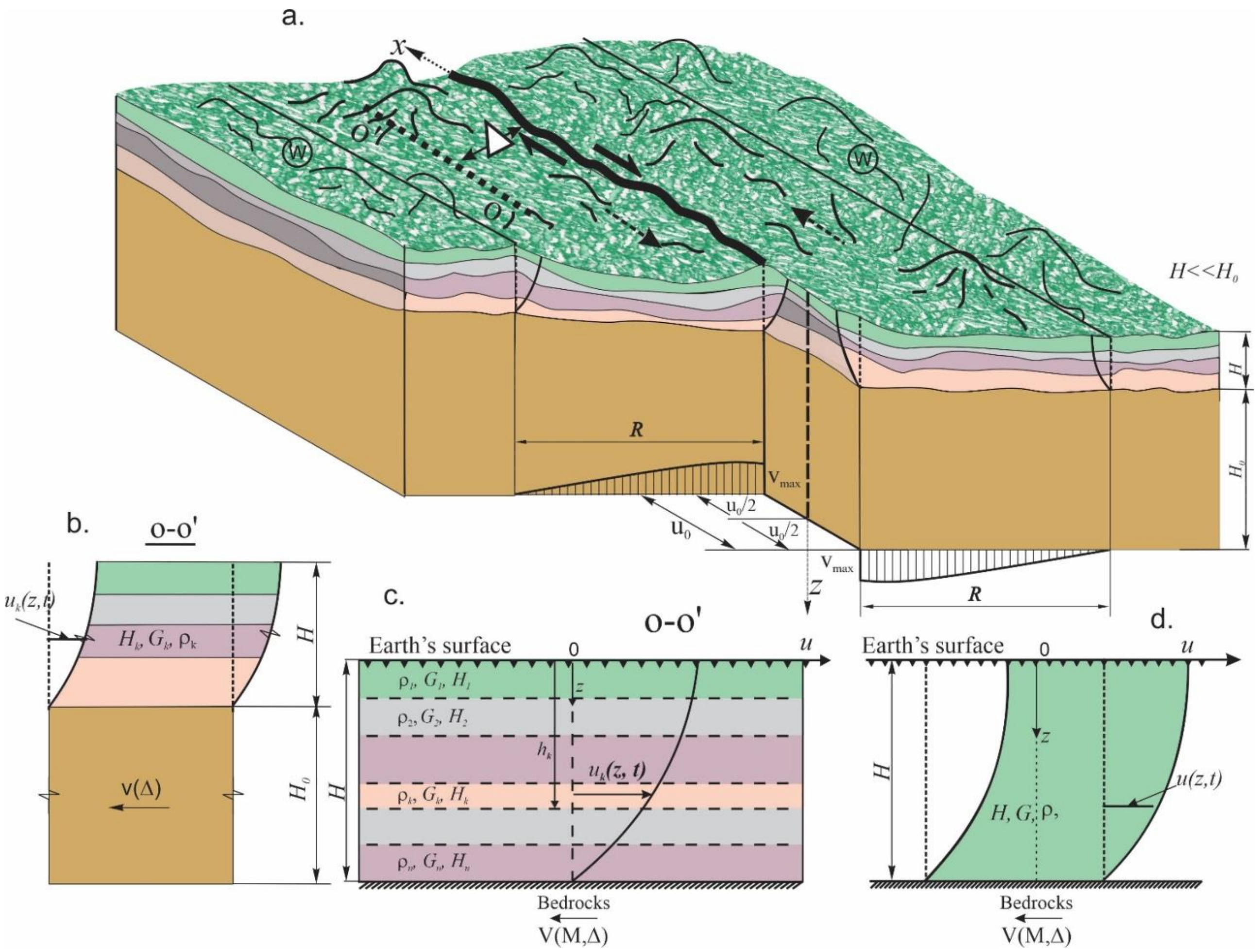

Figure 1. *Schematic diagram of the medium after an earthquake-caused rupture: a. diagram of the rupture and the mechanical model of the upper strata, b. the assumed structure of horizontal deformation in elevation view along the line O-O', c. diagram of the upper strata in the form of heterogeneous surface layer along the line O-O', d. the case of a homogenous near-surface layer;* u_0*-static deformation accumulated in the vicinity of the future rupture during the prolonged preparatory phase of the earthquake, R-the extent of the deformation zone in the direction perpendicular to the rupture, W- areas assumed to be undeformed by the impending earthquake: H - total thickness of the surface layer, Δ - distance from the rupture line to the observation point,* v_{max}*- velocity of the blocks at the rupture,* $v(M,\Delta)$ *- velocity of the blocks at the distance Δ from the rupture,* $u(z,t)$*- function of displacement in perpendicular direction relative to the rupture,* ρ_k*,* G_k*,* H_k*- density, shear modulus and thickness of the k-th layer,* $H+H_0$ *- depth of the rupture. Arrows indicate the blocks movement direction after rupture, the heavy line shows the rupture direction, dotted arrows show the direction of the layers' inertia movements after rupture (medium compression and dilatation).*

For the general case, during an earthquake (Figure 1) displacements functions of foundation bedding layers $u_k(z,t)$ must match the following wave equations [10, 11]:

$$G_k \frac{\partial^2 u_k}{\partial z^2} - \rho_k \frac{\partial^2 u_k}{\partial t^2} + \eta_k \frac{\partial^3 u_k}{\partial z^2 \partial t} = 0 \quad k = 1, 2 \ldots n \tag{1}$$

where G_k is the shear modulus of the k-th layer of the rocks, ρ_k is its density, η_k coefficient of viscosity (attenuation), H_k is thickness of the k-th layer, n is the number of layers. The value of initial velocity for the inertial movement of layers (which is equal to the after-rupture plate velocity, but in the opposite direction) is assumed as per the following formula [6]:

$$v(M,\Delta) = 100\, e^{M-8.5}\left(1 - \frac{\Delta^2}{R^2}\right) \tag{2}$$

Where M is the magnitude of the expected earthquake, Δ is the distance in kilometers from the site to the future rupture line, R is the length of the deformed area measured from the expected earthquake rupture. The values of the length R and average slip $\bar{u}$ (in meters) depending on the magnitude M are determined according to the following formulas [5]:

$$R = (5 \cdot \bar{u} + 15) \times 10^3, \ \lg \bar{u} = 0.55M - 3.71. \tag{3}$$

Data for predicted earthquake with values of $v(M,\Delta)$, R and ū are provided in Table 1, along with rock stratum ultimate (limit) shear strain values γ_{lim}, which were determined by the new methodology developed in [12], according to which the relationship between γ_{lim} and earthquake magnitude M is as follows:

$$10^4 \gamma_{\lim} = 0.39M - 2.23 \quad (4)$$

By assuming the solutions of the differential equation (1) as

$$u_k(z,t) = \sum_{i=1}^{\infty} U_{ki}(z) q_i(t), \qquad h_{k-1} \le U_{ki}(z) \le h_k,$$

$$h_0 = 0 \quad k = 1, 2 \ldots n, \quad (5)$$

and satisfying the boundary and initial conditions of the problem [3, 4], the following transcendental equation for multilayer system free oscillations frequencies and values of functions $U_{ki}(z)$ and $q_i(t)$ are obtained. The final values of displacements (seismograms) and accelerations (accelerograms) at the ground surface (z=0) would be as follows [6, 7]:

$$\begin{aligned} u_1(0,t) &= 100 e^{M-8.5}\left(1 - \frac{\Delta^2}{R^2}\right) \sum_{i=1}^{\infty} U_{1i}(0) \frac{T_{0i}}{2\pi} \delta_i e^{-n_i t} \sin\frac{2\pi}{T_{0i}} t \\ u_1''(0,t) &= 100 e^{M-8.5}\left(1 - \frac{\Delta^2}{R^2}\right) \sum_{i=1}^{\infty} U_{1i}(0) \frac{2\pi}{T_{0i}} \delta_i e^{-n_i t} \sin\frac{2\pi}{T_{0i}} t \end{aligned} \quad (6)$$

$$\delta_i = \frac{\sum_{k=1}^{n} \int_{h_{k-1}}^{h_k} \rho_k U_{ki}(z) dz}{\sum_{k=1}^{n} \int_{h_{k-1}}^{h_k} \rho_k U_{ki}^2(z) dz}, \quad h_0 = 0, \quad i = 1, 2, 3\ldots. \quad (7)$$

where $p_i = \frac{2\pi}{T_{0i}}$ is the angular frequency of the whole multilayer system's free oscillations derived from the relevant transcendental frequency equation, and n_i is the foundation bedding's attenuation coefficient for the *i*-th mode. Assuming $n_i^2 << p_i^2$, and $\eta_1 = \eta_2 = \eta$, while attenuation decrement Θ as being the same for all oscillation modes and equal to $\Theta = n_i T_{0i}$, where T_{0i} is the period of the *i*-th mode of the foundation bedding particles' oscillation mode as shear seismic waves propagate with a velocity of v_{Sk} in the layers of a heterogeneous foundation bedding, then the functions $U_{ki}(z)$ and $q_i(t)$ are as follows:

$$\begin{aligned} &U_{ki}(z) = A_{ki} \sin\lambda_{ki} z + B_{ki} \cos\lambda_{ki} z, \ k = 1.2\ldots n \\ &q_i(t) = e^{-n_i t}\left(c_{1i} \sin p_i^* t + c_{2i} \cos p_i^* t\right), \ i = 1, 2, 3\ldots \\ &\frac{p_i^2 \rho_k}{G_k} = \lambda_{ki}^2, \ \frac{p_i^2 \eta}{G_k} = 2n_i, \ p_i^* = \sqrt{p_i^2 - n_i^2} \approx p_i, \quad k = 1, 2\ldots n \end{aligned} \quad (8)$$

3. Natural Oscillation Modes of a Two-layer Foundation

Let us now focus in more detail on constructing synthetic seismograms and accelerograms for a two-layer foundation bedding, the schematic diagram of which is shown in Figure 2.

The equations of soil motion (1) for the two-layer foundation can be presented in the following form:

$$\begin{aligned} G_1 \frac{\partial^2 u_1}{\partial z^2} - \rho_1 \frac{\partial^2 u_1}{\partial t^2} + \eta_1 \frac{\partial^3 u_1}{\partial z^2 \partial t} = 0, \\ G_2 \frac{\partial^2 u_2}{\partial z^2} - \rho_2 \frac{\partial^2 u_2}{\partial t^2} + \eta_2 \frac{\partial^3 u_2}{\partial z^2 \partial t} = 0 \end{aligned} \quad (9)$$

Solutions of these equations by separation of variables can be presented as follows:

Table 1. *Values of the soil particles' oscillation velocities at the rupture* $v(M,\Delta)$ *in cm/sec, average slip* $\overline{u}$ *in meters, length of the deformed medium area* R *in km, and ultimate shear strain of ground* γ_{lim}, *depending on magnitude M and distance from the rupture* Δ *in km.*

Magnitude *M*	**Average slip, $\overline{u}$ m**	**The length of deformed area measured from the rupture line *R*, km**	**Rocks stratum ultimate (limit) shear strain values γ_{lim} x1(according to the formula (4)**	**Initial velocity at the rupture v_{max}, cm/sec, ($\Delta = 0$)**	**Values of soil particles' oscillation velocities $v(M,\Delta)$ in cm/sec depending on magnitude *M*, and distance from the rupture ($\Delta < R$) in km[1]**																						
					Values of Δ, in km																						
					2	**4**	**6**	**8**	**10**	**15**	**20 17 18 19**	**25 24 21**	**30 27**	**35 32**	**40 39**	**45**	**50 48**	**55**	**60 59**	**65 61**	**70**	**75**	**80 78**	**85**	**90**	**95**	**100 101**
6	0.39	16.9	0.11	8.2	8.1	7.7	7.2	6.4	5.3	1.7																	
6.25	0.54	17.7	0.21	10.5	10.4	10.0	9.3	8.4	7.2	3.0	0.8																
6.5	0.73	18.6	0.31	13.5	13.4	12.9	12.1	11.0	9.6	4.7	0.9																
6.75	1.00	20	0.40	17.4	17.2	16.7	15.8	14.6	13.0	7.6	1.7																
7	1.38	21.9	0.50	22.3	22.1	21.6	20.6	19.3	17.7	11.8	3.7	1.8															
7.25	1.90	24.3	0.60	28.7	28.5	27.9	26.9	25.5	23.8	17.7	9.2	0.7															
7.5	2.60	28	0.70	36.8	36.6	36.0	35.1	33.8	32.1	26.2	18.0	7.5	2.6														
7.75	3.57	32.8	0.79	47.2	47.1	46.5	45.7	44.4	42.8	37.4	29.7	19.8	7.7	2.3													
8	4.90	39.5	0.89	60.7	60.5	60.0	59.3	58.2	56.8	51.9	45.1	36.4	25.7	13.0	1.5												
8.25	6.73	48.6	0.99	77.9	77.7	77.4	76.7	75.8	74.6	70.5	64.7	57.3	48.2	37.5	25.1	11.1	1.9										
8.5	9.23	61.1	1.09	100.0	99.9	99.6	99.0	98.3	97.3	94.0	89.3	83.3	75.9	67.2	57.1	45.8	33.0	19.0	3.6	0.3							
8.75	12.68	78.4	1.18	128.4	128.3	128.1	127.7	127.1	126.3	123.7	120.0	115.3	109.6	102.8	95.0	86.1	76.2	65.2	53.2	40.1	26.0	10.9	1.3				
9	17.38	102	1.28	164.9	164.8	164.6	164.3	163.9	163.3	161.3	158.5	155.0	150.6	145.5	139.5	132.8	125.3	116.9	107.8	97.9	87.2	75.7	63.5	50.4	36.5	21.9	6.4 3.2

$$u(z,t)=\begin{cases} u_1(z,t)=\sum_{i=1}^{\infty}U_{1i}(z)q_i(t) & for\ \ 0\le z\le H_1 \\ u_2(z,t)=\sum_{i=1}^{\infty}U_{2i}(z)q_i(t) & for\ \ H_1\le z\le H \end{cases} \tag{10}$$

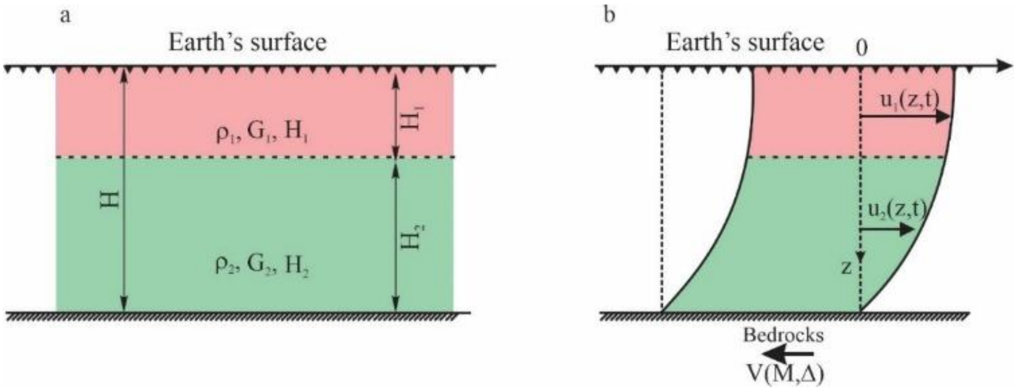

Figure 2. *The schematic diagram of an inertially deformed two-layer foundation bedding after a rupture.*

Inserting (10) and (9) and separating variables for the functions $U_{1i}(z)$ and $U_{2i}(z)$, as well as functions $q_i(t)$, the following equations are obtained [5]:

$$\begin{gathered} U''_{1i}(z)+\lambda_{1i}^2U_{1i}(z)=0,\ \ U''_{2i}(z)+\lambda_{2i}^2U_{2i}(z)=0, \\ \lambda_{1i}^2=\frac{p_i^2\rho_1}{G_1},\ \ \lambda_{2i}^2=\frac{p_i^2\rho_2}{G_2} \\ q''_i(t)+2n_iq'_i(t)+p_i^2q_i(t)=0, \\ \eta_1=\eta_2=\eta,\ \ \frac{\eta p_i^2}{G_k}=2n_i \end{gathered} \tag{11}$$

Solutions of the equations (11) are then presented in the following form:

$$\begin{aligned} &U_{1i}(z)=A_{1i}\sin\lambda_{1i}z+B_{1i}\cos\lambda_{1i}z, \\ &U_{2i}(z)=A_{2i}\sin\lambda_{2i}z+B_{2i}\cos\lambda_{2i}z \\ &q_i(t)=e^{-n_it}\left(c_{1i}\sin p_it+c_{2i}\cos p_it\right),\ \ i=1,2,3... \end{aligned} \tag{12}$$

where: n_i is the layers' attenuation coefficient for the i-th mode, p_i is the yet unknown angular frequency of the heterogeneous two-layer system's natural oscillations for the i-th mode, and A_{1i}, B_{1i}, A_{2i}, B_{2i}, c_{1i}, c_{2i} are unknown constants.

Satisfying the boundary conditions of medium continuity at the layers separation and the initial conditions which are as follows:

boundary condition:

for $z=0$ $\quad G_1\dfrac{\partial u_1(z,t)}{\partial z}=0$,

for $z=H_1+H_2$ $\quad u_2(z,t)=0$

medium continuity condition:

for $z=H_1$ $\quad u_1(z,t)=u_2(z,t)$,

$$G_1\frac{\partial u_1(z,t)}{\partial z}=G_2\frac{\partial u_2(z,t)}{\partial z} \tag{13}$$

initial conditions:

for $t=0$ $\quad u_k(z,t)=0,\ k=1,2$,

for $t=0$ $\quad \dfrac{\partial u_k(z,t)}{\partial t}=v(M.\Delta),\ \ k=1,2$,

The equations for determining values of all six coefficients A_{1i}, A_{2i}, B_{1i}, B_{2i} and c_{1i}, c_{2i} can be obtained. Using the first four boundary and continuity conditions (13), for coefficients A_{1i}, A_{2i}, B_{1i}, B_{2i}, the following system of algebraic homogeneous equations can be obtained:

$$\begin{gathered} A_{1i}=0 \\ A_{2i}\sin\lambda_{2i}H+B_{2i}\cos\lambda_{2i}H=0 \\ A_{1i}\sin\lambda_{1i}H_1+B_{1i}\cos\lambda_{1i}H_1=A_{2i}\sin\lambda_{2i}H_1+B_{2i}\cos\lambda_{2i}H_1 \\ A_{1i}G_1\lambda_{1i}\cos\lambda_{1i}H_1-B_{1i}G_1\lambda_{1i}\sin\lambda_{1i}H_1= \\ =A_{2i}G_2\lambda_{2i}\cos\lambda_{2i}H_1-B_{2i}G_2\lambda_{2i}\sin\lambda_{2i}H_1 \end{gathered} \tag{14}$$

By setting to zero the fourth-degree determinant of the system of four homogeneous equations (14) with respect to the coefficients A_{1i}, A_{2i}, B_{1i}, B_{2i}, the following equation for determining the frequency spectrum $p_i = \frac{2\pi}{T_{0i}}$ is obtained, included in coefficients λ_{1i} and λ_{2i} of the formula (11):

$$\begin{vmatrix} 1 & 0 & 0 & 0 \\ 0 & 0 & \sin\lambda_{2i}(H_1+H_2) & \cos\lambda_{2i}(H_1+H_2) \\ \sin\lambda_{1i}H_1 & \cos\lambda_{1i}H_1 & -\sin\lambda_2 H_1 & -\cos\lambda_{2i}H_1 \\ G_1\lambda_{1i}\cos\lambda_{1i}H_1 & -G_1\lambda_{1i}\sin\lambda_1 H_1 & -G_2\lambda_{i2}\cos\lambda_{2i}H_1 & G_2\lambda_{2i}\sin\lambda_{2i}H_1 \end{vmatrix} = 0 \quad (15)$$

By expanding (15) the following transcendental equation for frequencies is derived:

$$\sqrt{\frac{\rho_1 G_1}{\rho_2 G_2}} tg \frac{2\pi H_1}{T_{0i}} \sqrt{\frac{\rho_1}{G_1}} \cdot tg \frac{2\pi H_2}{T_{0i}} \sqrt{\frac{\rho_2}{G_2}} - 1 = 0 \quad (16)$$

The values of coefficients A_{1i}, A_{2i}, B_{1i}, B_{2i} and functions $U_{1i}(z)$, $U_{2i}(z)$ would then be in the following form:

$$\begin{aligned} &A_{1i} = 0 \\ &A_{2i} = -B_{1i}\frac{\cos\lambda_{1i}H_1}{\sin\lambda_{2i}H_2}\cos\lambda_{2i}(H_1+H_2), \\ &U_{1i}(z) = B_{1i}\cos\frac{2\pi z}{T_{0i}v_{S1}}, \quad \lambda_{1i} = \frac{2\pi}{T_{0i}}\cdot\frac{1}{v_{S1}} \\ &B_{2i} = B_{1i}\frac{\cos\lambda_{1i}H_1}{\sin\lambda_{2i}H_2}\sin\lambda_{2i}(H_1+H_2), \\ &U_{2i}(z) = -B_{1i}\frac{\cos\lambda_{1i}H_1}{\sin\lambda_{2i}H_2}\sin\frac{2\pi(z-H)}{T_{0i}v_{S2}}, \quad \lambda_{2i} = \frac{2\pi}{T_{0i}}\cdot\frac{1}{v_{S2}} \end{aligned} \quad (17)$$

Based on the last two equations for initial conditions (13), to determine c_{1i}, c_{2i}, the following is derived:

$$\begin{aligned} &\sum_{i=1}^{\infty} U_{ki}(z)\cdot 1\cdot(c_{1i}\cdot 0 + c_{2i}\cdot 1) = 0, \; k = 1,2, \\ &\sum_{i=1}^{\infty} U_{ki}(z)\cdot 1\cdot(c_{1i}\cdot p_i\cdot 1 - n\cdot 1\cdot 0) = v(M,\Delta), \; k = 1,2 \end{aligned} \quad (18)$$

Since the first condition (18) must hold true for any point z along the height of the two-layer lithological column, and the coefficients A_{ki}, B_{ki} ($k = 1,2$) cannot both be zero simultaneously, it follows from (18) that:

$$c_{2i} = 0, \quad i = 1,2,3... \quad (19)$$

The second equation of (18) can be used to derive the following two equations:

$$\sum_{i=1}^{\infty} U_{1i}(z)\, p_i c_{1i} = v(M,\Delta), \text{ and } \sum_{i=1}^{\infty} U_{2i}(z)\, p_i c_{1i} = v(M,\Delta), \quad (20)$$

If each of the equations (20) is multiplied by $\rho_1 U_{1j}(z)$ and $\rho_2 U_{2j}(z)$, respectively, and integrated between 0 and H, according to (10) replaced beforehand by the sum of integrals between т 0 and H_1, and between H_1 and H_1+H_2, then using simple transformations the following single equation can be derived from the two new expressions (20):

$$\begin{aligned} &p_i c_{1i}\left[\int_0^{H_1}\sum_{i=1}^{\infty}\rho_1 U_{1i}(z)U_{1j}(z)dz + \int_{H_1}^{H_1+H_2}\sum_{i=1}^{\infty}\rho_2 U_{2i}(z)U_{2j}(z)dz\right] = \\ &= v(M,\Delta)\left[\int_0^{H_1}\rho_1 U_{1j}(z)dz + \int_{H_1}^{H_1+H_2}\rho_2 U_{2j}(z)dz\right] \end{aligned} \quad (21)$$

Considering that the functions U_{ki} and U_{kj} are orthogonal [13];

$$\int_0^{H_1}\rho_1 U_{1i}(z)U_{1j}(z)dz + \int_{H_1}^{H_1+H_2}\rho_2 U_{2i}(z)U_{2j}(z)dz = 0 \quad (22)$$

then under $i \neq j$ for all combinations of i-th and j-th oscillation modes, the following is derived from (21):

$$p_i c_{1i}\left[\int_0^{H_1}\rho_1 U_{1i}^2(z)\,dz+\int_{H_1}^{H_1+H_2}\rho_2 U_{2i}^2(z)\,dz\right]= \\ =v(M,\Delta)\left[\int_0^{H_1}\rho_1 U_{1i}(z)\,dz+\int_{H_1}^{H_1+H_2}\rho_2 U_{2i}(z)\,dz\right] \qquad (23)$$

Therefore, for the coefficients c_{1i} and c_{2i} the following is holds:

$$c_{2i}=0,$$

$$c_{1i}=\frac{v(M,\Delta)\left(\int_0^{H_1}\rho_1 U_{1i}(z)\,dz+\int_{H_1}^{H_1+H_2}\rho_2 U_{2i}(z)\,dz\right)}{p_i\left(\int_0^{H_1}\rho_1 U_{1i}^2(z)\,dz+\int_{H_1}^{H_1+H_2}\rho_2 U_{2i}^2(z)\,dz\right)}, \qquad (24)$$

$$i=1,2,3...$$

The final expressions for displacements and accelerations (i.e. $u_1(0,t)$ and $u_1''(0,t)$) at ground surface (z=0 and assuming that the attenuation coefficient values n_i are small compared to $e^{-n_i t}$) according to formulas (2), (10), (12), (17) and (24) will be:

$$u_1(0,t)=100\,e^{M-8.5}\left(1-\frac{\Delta^2}{R^2}\right)\sum_{i=1}^{\infty}U_{1i}(0)\frac{T_{0i}}{2\pi}\delta_i e^{-n_i t}\sin\frac{2\pi}{T_{0i}}t \\ u_1''(0,t)=100\,e^{M-8.5}\left(1-\frac{\Delta^2}{R^2}\right)\sum_{i=1}^{\infty}U_{1i}(0)\frac{2\pi}{T_{0i}}\delta_i e^{-n_i t}\sin\frac{2\pi}{T_{0i}}t \qquad (25)$$

where δ_i represents:

$$\delta_i=\frac{\rho_1\int_0^{H_1}U_{1i}(z)\,dz+\rho_2\int_{H_1}^{H_1+H_2}U_{2i}(z)\,dz}{\rho_1\int_0^{H_1}U_{1i}^2(z)\,dz+\rho_2\int_{H_1}^{H_1+H_2}U_{2i}^2(z)\,dz},\quad i=1,2,3... . \qquad (26)$$

Inserting the values of $U_{1i}(z)$ and $U_{2i}(z)$ from (17) into (26) and integrating it for δ_i, the following is derived:

$$\delta_i=4\cdot\frac{\rho_1\frac{v_{S1}}{v_{S2}}\sin\frac{2\pi H_1}{T_{0i}v_{S1}}+\rho_2\frac{\cos\frac{2\pi H_1}{T_{0i}v_{S1}}}{\sin\frac{2\pi H_2}{T_{0i}v_{S2}}}\cdot\left(1-\cos\frac{2\pi H_2}{T_{0i}v_{S2}}\right)}{B_{1i}\left[\rho_1\frac{v_{S1}}{v_{S2}}\left(\frac{4\pi H_1}{T_{0i}v_{S1}}+\sin\frac{4\pi H_1}{T_{0i}v_{S1}}\right)+\rho_2\left(\frac{\cos\frac{2\pi H_1}{T_{0i}v_{S1}}}{\sin\frac{2\pi H_2}{T_{0i}v_{S2}}}\right)^2\left(\frac{4\pi H_2}{T_{0i}v_{S2}}-\sin\frac{4\pi H_2}{T_{0i}v_{S2}}\right)\right]}, \qquad (27)$$

$$i=1,2,3...$$

Values of the constant B_{1i} can be assumed to be equal to 1 ($B_{1i}=1$), because considering formulas (17) and (27), the final forms of (25) for seismograms and accelerograms $u_1(0,t)$ and $u_1''(0,t)$, the values of B_{1i} will cancel out.

In a particular case, taking:

$$H_1=0,\ v_s=0,\ H_2=H,\ v_{s2}=v_s,\ \rho_1=0,$$

$$\rho_2=\rho,\ T_{0i}=\frac{4H}{(2i-1)v_s},\quad i=1,2,3...$$

From expression (27) we obtain:

$$\delta_i=4\cdot\frac{0+\rho\frac{1}{(-1)^{i-1}}\cdot\left(1-\cos(2i-1)\frac{\pi}{2}\right)}{0+\rho\cdot 1\left(\frac{4\pi H v_s}{4H v_S}(2i-1)-\sin\pi(2i-1)\right)}=\frac{4(-1)^{i+1}}{\pi(2i-1)},$$

which coincides with the expression derived for a homogeneous base in [5, 6].

Seismograms and accelerograms of two-layer and their equivalent single-layer foundation beddings at the Earth's *surface*.

The 16 variants of heterogeneous foundation beddings are considered, the main parameters of which are presented in Figure 2 and Tables 2 and 3, where H_1 and H_2, v_{S1} and v_{S2}, ρ_1 and ρ_2 are thicknesses, propagation velocities of seismic shear waves and ground layer densities, respectively. The first three oscillation periods T_{01}, T_{02} and T_{03} for all 16 heterogeneous beddings are also presented in Tables 2 and 3, which are derived from the transcendental equations of frequencies (16), while the values of coefficients δ_i are obtained from the formula (27).

Table 2 also provides the physical and mechanical characteristics for all equivalent homogeneous foundation beddings: average values of propagation velocity of displacement waves.

Table 2. *Physical and mechanical properties of heterogeneous foundation beddings.*

Heterogeneous foundation beddings													
No.	**v_{s1}, cm/s**	**H_1, m**	**ρ_1, t∗cm^2/m^4**	**v_{s2}, cm/s**	**H_2, m**	**ρ_2, t∗cm^2/m^4**	**v_{s1}/v_{s2}**	**Derived from the formula (16), in seconds**			**Derived by the formula (27)**		
								T_{01},	**T_{02},**	**T_{03},**	**δ_1**	**δ_2**	**δ_3**
1.	400	10	0.2	600	20	0.22	0.67	0.207	0.073	0.047	1.891	-0.522	0.483
2.	250	10	0.2	600	20	0.22	0.42	0.232	0.107	0.056	1.865	-0.873	0.861
3.	200	10	0.2	400	20	0.22	0.50	0.380	0.151	0.080	1.723	-0.701	0.714
4.	150	10	0.2	300	20	0.2	0.50	0.458	0.190	0.100	1.842	-0.787	0.498
5.	150	15	0.2	250	15	0.22	0.60	0.657	0.191	0.127	2.095	-1.000	0.704
6.	125	15	0.2	200	15	0.2	0.63	0.925	0.308	0.154	1.903	-0.488	0.486
7.	100	5	0.18	600	25	0.22	0.17	0.246	0.145	0.069	1.256	-1.104	0.867
8.	600	25	0.22	100	5	0.18	6.00	0.740	0.107	0.079	6.329	-0.126	0.330
9.	530	13	0.22	600	17	0.22	0.88	0.203	0.071	0.042	2.250	-0.612	0.465
10.	620	14	0.22	700	16	0.22	0.89	0.174	0.061	0.036	2.406	-0.631	0.510
11.	340	18	0.2	400	12	0.2	0.85	0.245	0.098	0.063	3.491	-1.105	0.346
12.	450	14	0.22	550	16	0.22	0.82	0.336	0.074	0.054	1.789	-0.672	0.346
13.	280	16.5	0.2	350	13.5	0.22	0.80	0.365	0.132	0.078	2.729	-0.813	0.688
14.	150	15	0.2	200	15	0.22	0.75	0.667	0.222	0.138	2.442	-0.816	0.623
15.	208	20	0.2	150	12	0.2	1.39	0.785	0.228	0.143	3.282	-0.587	0.443
16.	200	4.8	0.1626	300	30.7	0.1775	0.67	0.469	0.160	0.100	1.241	-0.604	0.437
17.	400	20	0.22	125	10	0.18	3.20	0.438	0.162	0.103	5.371	-0.115	0.416
18.	530	13	0.22	280	17	0.22	1.89	0.164	0.047	0.026	2.461	-0.347	0.085

Table 2. *Continued.*

Equivalent homogeneous beddings													
No.	**v_{s1}, cm/s**	**H_1, m**	**ρ_1, t∗cm^2/m^4**	**v_{s2}, cm/s**	**H_2, m**	**ρ_2, t∗cm^2/m^4**	**Derived by the formulas (28), (29), (30)**						
							$\bar{v}_s$, cm/s	**$\bar{T}_{01}$, s**	**$\bar{T}_{02}$, s**	**$\bar{T}_{03}$, s**	**$\bar{\delta}_1$**	**$\bar{\delta}_2$**	**$\bar{\delta}_3$**
1.	400	10	0.2	600	20	0.22	514	0.233	0.078	0.047	1.274	-0.425	0.255

Equivalent homogeneous beddings

No.	v_{s1}, cm/s	H_1, m	ρ_1, t*cm²/m⁴	v_{s2}, cm/s	H_2, m	ρ_2, t*cm²/m⁴	Derived by the formulas (28), (29), (30)						
							$\overline{v}_s$, cm/s	$\overline{T}_{01}$, s	$\overline{T}_{02}$, s	$\overline{T}_{03}$, s	$\overline{\delta}_1$	$\overline{\delta}_2$	$\overline{\delta}_3$
2.	250	10	0.2	600	20	0.22	409	0.293	0.098	0.059	1.274	-0.425	0.255
3.	200	10	0.2	400	20	0.22	300	0.400	0.133	0.080	1.274	-0.425	0.255
4.	150	10	0.2	300	20	0.2	225	0.533	0.178	0.107	1.274	-0.425	0.255
5.	150	15	0.2	250	15	0.22	187	0.640	0.213	0.128	1.274	-0.425	0.255
6.	125	15	0.2	200	15	0.2	153	0.780	0.260	0.156	1.274	-0.425	0.255
7.	100	5	0.18	600	25	0.22	327	0.367	0.122	0.073	1.274	-0.425	0.255
8.	600	25	0.22	100	5	0.18	327	0.367	0.122	0.073	1.274	-0.425	0.255
9.	530	13	0.22	600	17	0.22	567	0.211	0.070	0.042	1.274	-0.425	0.255
10.	620	14	0.22	700	16	0.22	660	0.182	0.061	0.036	1.274	-0.425	0.255
11.	340	18	0.2	400	12	0.2	361	0.332	0.111	0.066	1.274	-0.425	0.255
12.	450	14	0.22	550	16	0.22	498	0.241	0.080	0.048	1.274	-0.425	0.255
13.	280	16.5	0.2	350	13.5	0.22	307	0.390	0.130	0.078	1.274	-0.425	0.255
14.	150	15	0.2	200	15	0.22	171	0.700	0.233	0.140	1.274	-0.425	0.255
15.	208	20	0.2	150	12	0.2	181	0.705	0.235	0.141	1.274	-0.425	0.255
16.	200	4.8	0.1626	300	30.7	0.1775	281	0.505	0.168	0.101	1.274	-0.425	0.255

Note: Variants 7 and 8 are excluded because the physical and mechanical properties of their layers significantly differ from each other, and averaging is not applicable.

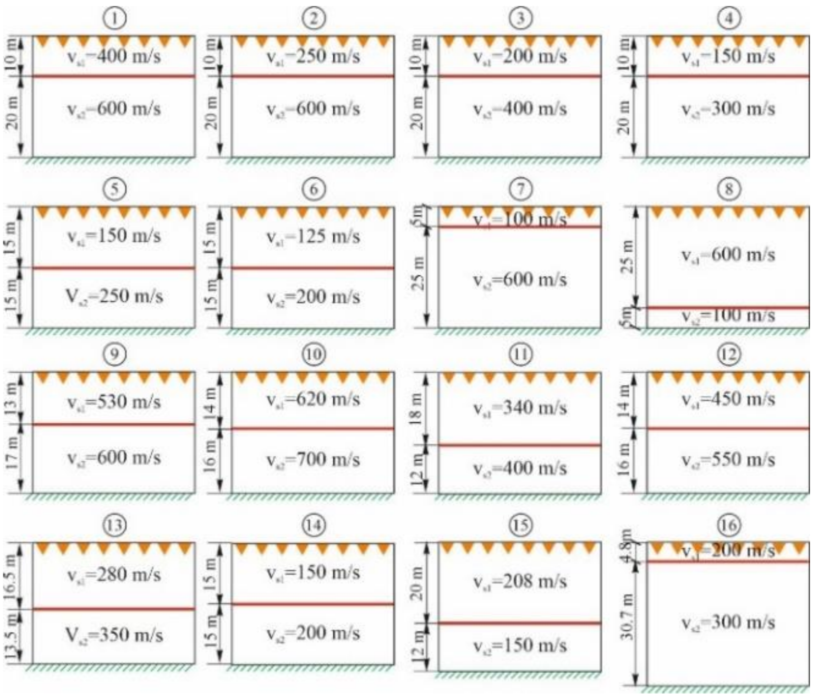

Figure 3*. Diagrams of the considered heterogeneous foundation eddings[2].*

***Table 3.** Comparative characteristics of the oscillation periods and modes for heterogeneous and equivalent homogeneous foundation beddings.*

No.	Two-layer heterogeneous foundation beddings						Equivalent single-layer homogeneous beddings				Comparative ratios of the parameters					
	T_{01}, s[3]	δ1	δ2	δ3	$\frac{\delta_1}{\delta_2}$	$\frac{\delta_1}{\delta_3}$	$\bar{T}_{01}$, s	$\bar{\delta}$1	$\bar{\delta}$2	$\bar{\delta}$3	$\frac{\bar{T}_{01}}{T_{01}}$	$\frac{\bar{T}_{02}}{T_{02}}$	$\frac{\bar{T}_{03}}{T_{03}}$	$\frac{\delta_1}{\bar{\delta}_1}$	$\frac{\delta_2}{\bar{\delta}_2}$	$\frac{\delta_3}{\bar{\delta}_3}$
1	0.207	1.890	-0.522	0.483	3.62	3.92	0.233	1.274	-0.424	0.254	1.127	1.07	0.99	1.483	1.230	1.894
2	0.232	1.865	-0.873	0.861	2.14	2.17	0.293	1.274	-0.424	0.254	1.266	0.92	1.04	1.464	2.056	3.380
3	0.380	1.723	-0.701	0.714	2.46	2.41	0.400	1.274	-0.424	0.254	1.053	0.88	1.00	1.352	1.650	2.802
4	0.458	1.842	-0.787	0.498	2.34	3.70	0.533	1.274	-0.424	0.254	1.164	0.94	1.07	1.446	1.853	1.954
5	0.657	2.095	-1.000	0.704	2.10	2.98	0.640	1.274	-0.424	0.254	0.974	1.12	1.01	1.645	2.355	2.762
6	0.925	1.903	-0.488	0.486	3.90	3.91	0.780	1.274	-0.424	0.254	0.843	0.84	1.01	1.494	1.150	1.909
7	0.246	1.256	-1.104	0.867	1.14	1.45	0.367	1.274	-0.424	0.254	1.492	0.85	1.07	0.986	2.600	3.402
8	0.740	6.329	-0.126	0.330	50.1	19.15	0.367	1.274	-0.424	0.254	0.495	1.15	0.92	4.968	0.298	1.297
9	0.203	2.250	-0.612	0.465	3.67	4.84	0.211	1.274	-0.424	0.254	1.042	0.99	1.01	1.766	1.442	1.823
10	0.174	2.406	-0.631	0.510	3.81	4.72	0.182	1.274	-0.424	0.254	1.044	0.99	1.01	1.889	1.487	2.000
11	0.245	3.491	-1.105	0.346	3.16	10.09	0.332	1.274	-0.424	0.254	1.354	1.13	1.05	2.740	2.602	1.358
12	0.336	1.789	-0.672	0.346	2.66	5.17	0.241	1.274	-0.424	0.254	0.718	1.08	0.90	1.404	1.583	1.357
13	0.365	2.729	-0.813	0.688	3.36	3.96	0.390	1.274	-0.424	0.254	1.069	0.99	1.00	2.142	1.915	2.702
14	0.667	2.442	-0.816	0.623	2.99	3.92	0.700	1.274	-0.424	0.254	1.050	1.05	1.02	1.917	1.921	2.445
15	0.785	3.282	-0.587	0.443	5.59	7.41	0.705	1.274	-0.424	0.254	0.898	1.03	0.98	2.576	1.382	1.739
16	0.469	1.241	-0.604	0.437	2.05	2.84	0.505	1.274	-0.424	0.254	1.076	1.05	1.01	0.974	1.423	1.716
Average value excludes Nos. 7 and 8[4]					3.1	4.4					1.05	1.01	1.01	1.74	1.72	2.13

$\bar{v}_S$ and densities $\bar{\rho}$, which are determined by the following formulas [6]:

$$\bar{v}_S = \frac{H_1 + H_2}{\frac{H_1}{v_{s1}} + \frac{H_2}{v_{s2}}}, \quad \bar{\rho} = \frac{H_1\rho_1 + H_2\rho_2}{H_1 + H_2} \tag{28}$$

Values of the equivalent homogeneous foundation bedding first period are determined by the following formula:

$$\bar{T}_0 = \frac{4(H_1 + H_2)}{\bar{v}_s} \tag{29}$$

whereas values of the next periods $\bar{T}_{0i}$ (i=1,2,3…) and coefficients $\bar{\delta}_i$ (i=1,2,3…) are assumed by the formulas for a homogeneous foundation bedding [9]:

$$\bar{T}_{0i} = \frac{\bar{T}_{01}}{2i-1}, \ i=1,2,3\ldots, \quad \bar{\delta}_i = \frac{4}{\pi}\cdot\frac{(-1)^{i+1}}{2i-1}, \ i=1,2,3\ldots. \tag{30}$$

Figure 4 presents the first three natural oscillation modes of heterogeneous beddings based on formulas (16), (17) and respective equivalent homogeneous beddings for all variants of heterogeneous beddings.

Table 4 presents the final results of calculations according to formulas (25) for peak ground displacements and accelerations under M=7.0, Δ=15 km, and ground vibration decrement $\Theta = n_i T_{0i} = 0.3$ for all five modes of oscillation, which corresponds to 4.77% of critical attenuation $n_{.ic.} = p_i$. Based on the vibration decrement formula Θ [7], the following ratios between n% and Θ are set:

$$n\% = \frac{100\Theta}{2\pi}, \quad \Theta = \frac{2\pi \cdot n\%}{100} \tag{31}$$

As seen in the table, when replacing heterogeneous bedding with an equivalent homogeneous one, the best approximation for ground accelerations u''_{0max} and $\overline{u}''_{0max}$ occurs when the accelerograms of the equivalent heterogeneous bedding are calculated factoring in five modes of oscillation, while for the heterogeneous bedding, with three modes.

Figure 4 shows superposition of the first three oscillation modes for heterogeneous (a)) and equivalent homogeneous (b)) foundation beddings. As it is apparent, unlike with homogeneous bedding, for the heterogeneous one, individual oscillation modes peak occurrences differ in time, but this does not result in significant increases.

The results presented in Table 4 also show that for a heterogeneous bedding, the values of u_1 and u''_1 are significantly greater than the values of $\overline{u}_1$ and $\overline{u}''_1$ for a homogeneous bedding. This outcome is related to the ratios of the coefficients $\delta_i(i = 1,2,3\ldots)$ in the main formula (25) for predicted values of heterogeneous bedding seismograms and accelerograms, to the similar coefficients $\bar{\delta}_i(i = 1,2,3\ldots)$ for the homogeneous bedding, as given in Table 3. As seen in the table, the average values of $\delta_i/\bar{\delta}_i$ for the first, second, and third oscillation modes reach approximately 1.74, 1.72, and 2.13, respectively. Furthermore, Table 3 shows that the average ratios of the first periods $\overline{T}_{01}$ and T_{01} are about 1.05, while the ratios $\overline{T}_{02}$ to T_{02}, and $\overline{T}_{03}$ to T_{03} are approximately 1.01; these values also are part of the main prediction formula (25). This indicates that the values of seismograms and accelerograms calculated for a heterogeneous foundation using the main formula (25) will be primarily influenced by the coefficients δ_i and $\bar{\delta}_i$, rather than by the values of T_{0i} and $\overline{T}_{0i}$, which are also part of the main formula (25). Seismograms and accelerograms for the 16 variants (Figure 3) are shown in Figure 5.

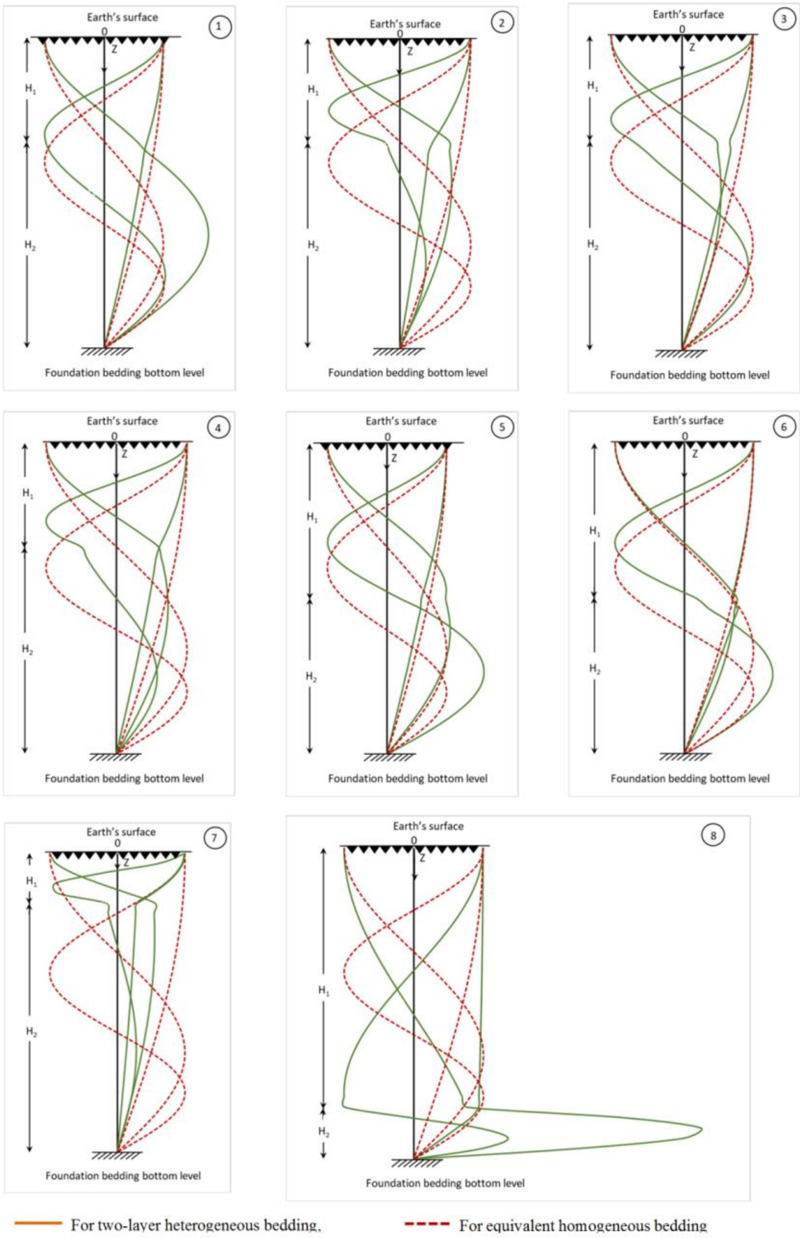

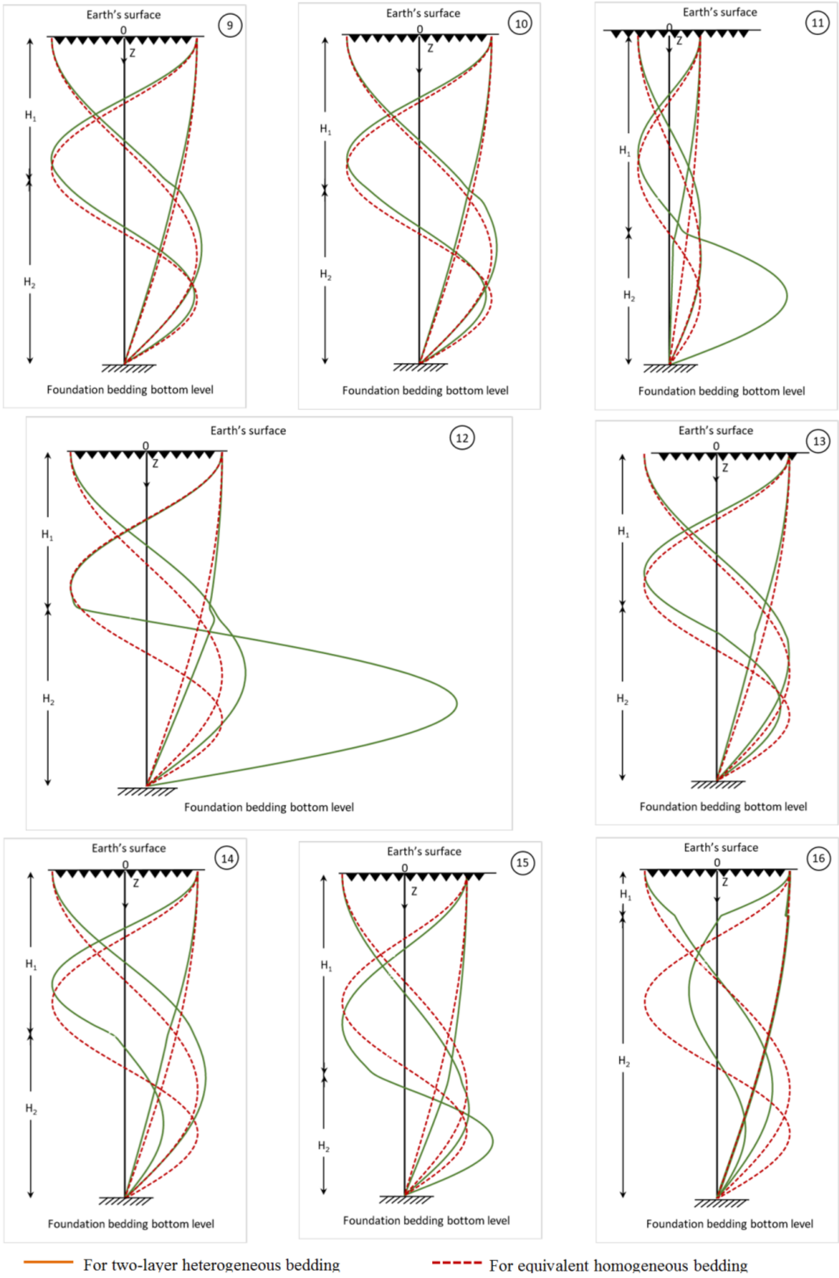

Figure 4. *The first three natural oscillation modes of two-layer and equivalent homogeneous beddings, according to the diagrams of Figure 3.*

As shown in Figure 3, the degree of foundation bedding heterogeneity depends mainly on differences in shear wave velocity v_s between the first and second layers. For two-layer heterogeneous bedding cases where $v_{s1} < v_{s2}$, the increase in acceleration values (accelerograms) in the first layer (at the Earth's surface, *z*=0) is similar to the problem with a structure vibrating with two degrees of freedom, an effect previously noted by Biot [14] and termed the "whip effect." In these cases, the wave propagating from the lower to the upper layer can be viewed as energy flow moving from the heavier (stiffer) part of the whip to the lighter (more flexible) part, causing energy accumulation in the small mass of the upper flexible layer and resulting in large accelerations. For two heterogeneous beddings (8), (16) where $v_{s2} < v_{s1}$, this is akin to the seismic response of buildings supported by special seismic isolators, where the building as a whole undergoes large displacements (rather than deformations) with minimal floor drifts.

Table 4. Peak values of synthetic seismograms and accelerograms for 16 heterogeneous beddings and equivalent homogeneous beddings based on the formula (25).

No.	Heterogeneous beddings			Equivalent homogeneous bedding					Ratios of heterogeneous bedding actual displacements and accelerations with consideration of three oscillations modes relative to the equivalent with five oscillations modes	
	First oscillation mode period T_{01}, s	Actual values of displacements and accelerations with consideration of three oscillations modes according to the formula (25)		Average values of the first oscillation mode period $\overline{T}_{01}$, sec	Equivalent values of displacements and accelerations with consideration of three oscillations modes		Equivalent values of displacements and accelerations with consideration of five oscillations modes			
		$u_{1\max}(0)$, cm	$u''_{1max}(0)$, cm/s2		$\overline{u}_{1\max}(0)$, cm	$\overline{u}''_{1max}(0)$, cm/s2	$\overline{u}_{1max}(0)$, cm	$\overline{u}''_{1max}(0)$, cm/s2	$\frac{u_{1\max}(0)}{\overline{u}_{1max}(0)}$	$\frac{u''_{1max}(0)}{\overline{u}''_{1max}(0)}$
1	0.207	0.75	1482	0.233	0.58	965	0.591	1374	1.27	1.08
2	0.232	0.88	1714	0.293	0.73	768	0.745	1077	1.18	1.59
3	0.380	1.35	1008	0.400	1.00	572	1.021	833	1.32	1.21
4	0.458	1.70	737	0.533	1.34	428	1.361	617	1.25	1.19
5	0.657	2.79	782	0.640	1.61	357	1.634	520	1.71	1.50
6	0.925	3.35	370	0.780	1.96	292	1.991	421	1.68	0.88
7	0.246	0.63	1173	0.367	0.92	623	0.937	901	0.67	1.30
8	0.740	8.24	794	0.367	0.92	623	0.937	901	8.79	0.88
9	0.203	0.89	1799	0.211	0.53	1057	0.535	1460	1.66	1.23
10	0.174	0.80	1959	0.182	0.44	1085	0.444	1266	1.80	1.55
11	0.245	1.62	1796	0.332	0.83	682	0.846	970	1.91	1.85
12	0.336	1.08	1049	0.241	0.60	950	0.615	1383	1.76	0.76
13	0.365	1.95	1309	0.390	0.97	579	0.990	829	1.97	1.58
14	0.667	3.23	699	0.700	1.76	325	1.786	467	1.81	1.50
15	0.785	4.77	592	0.705	1.77	321	1.797	462	2.65	1.28
16	0.469	1.09	619	0.505	1.26	445	1.283	635	0.85	0.97
17	0.438	0.356	299							
18	0.167	0.726	1451							
Average value without Nos. 7 and 8									1.63	1.3

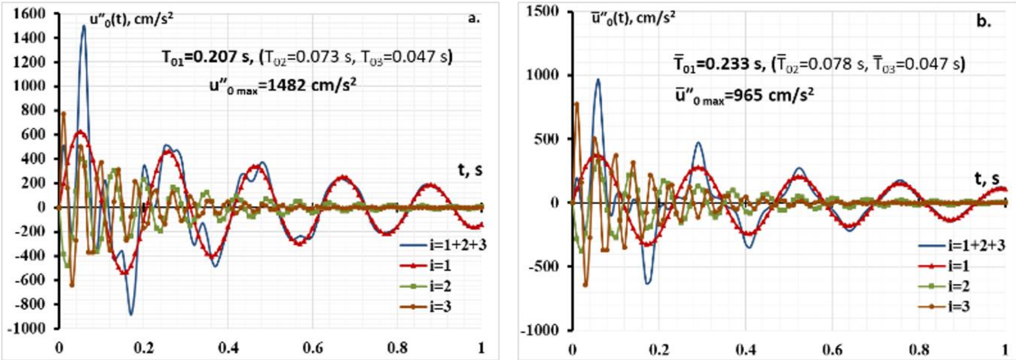

Figure 5. *Superposition of acceleration values for the first three oscillation modes (at ground surface) according to the formula (25), at M=7.0, Δ=15 km, $\Theta_1=\Theta_2=\Theta_3=0.3$: for individual oscillation modes (first i=1, second i=2, and third i=3), and their sum (i=1+2+3)): a. for No. 1 variant of heterogeneous foundation bedding with* $T_{01} = 0.208\ sec$, $\delta_1 = 1.890$ *b. for the equivalent homogeneous bedding with average value* $\overline{T}_{01} = 0.233\ sec, \bar{\delta}_1 = 1.227$*(b).*

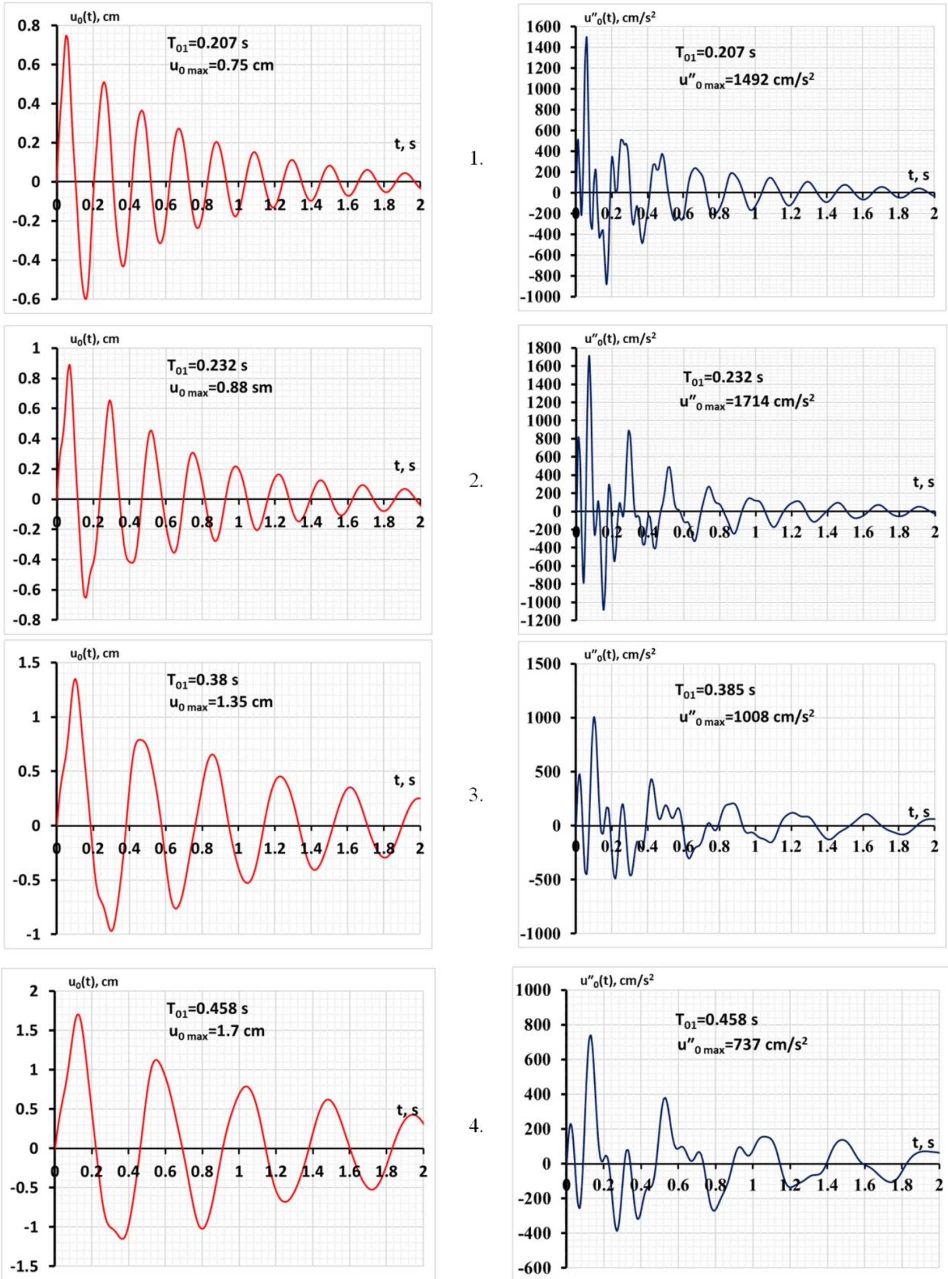

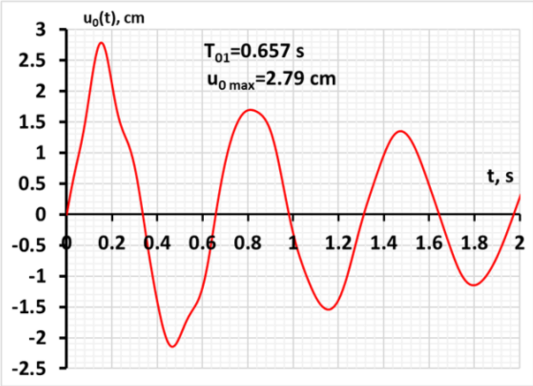
u0(t), cm
T01=0.657 s
u0 max=2.79 cm
t, s

5.

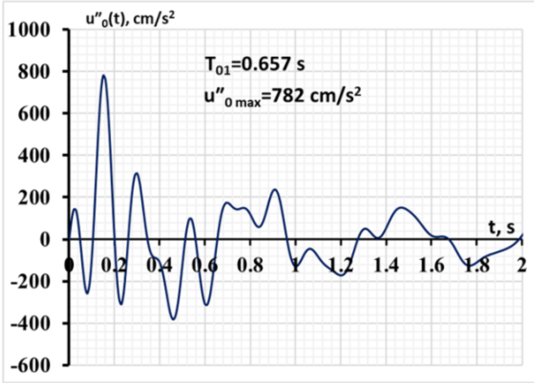
u"0(t), cm/s2
T01=0.657 s
u"0 max=782 cm/s2
t, s

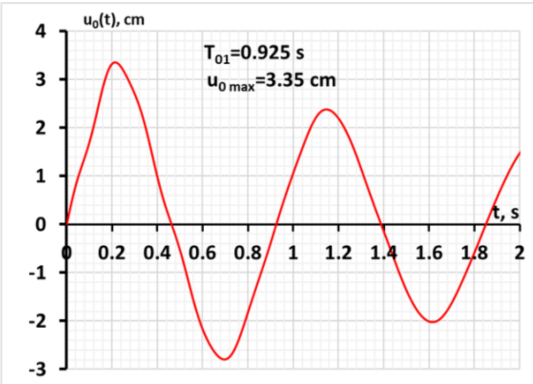
u0(t), cm
T01=0.925 s
u0 max=3.35 cm
t, s

6.

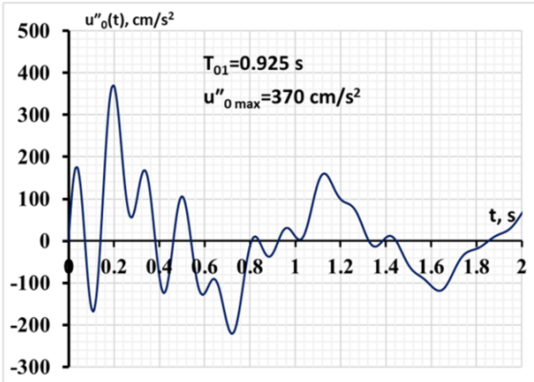
u"0(t), cm/s2
T01=0.925 s
u"0 max=370 cm/s2
t, s

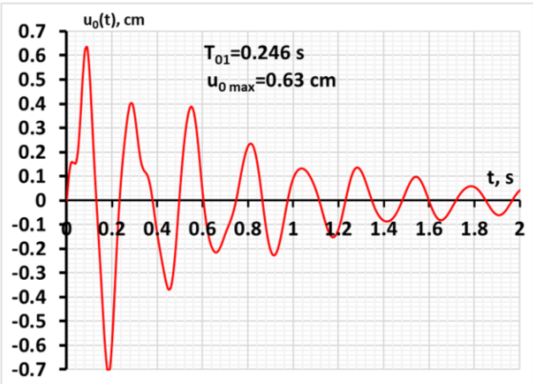
u0(t), cm
T01=0.246 s
u0 max=0.63 cm
t, s

7.

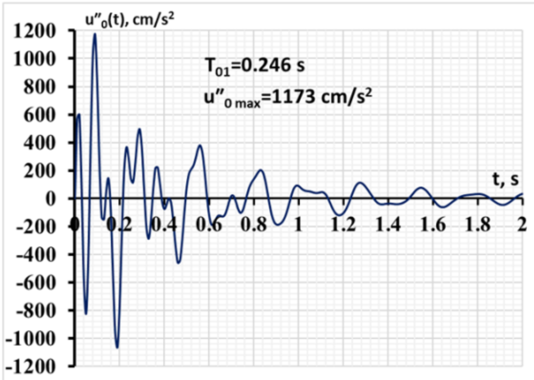
u"0(t), cm/s2
T01=0.246 s
u"0 max=1173 cm/s2
t, s

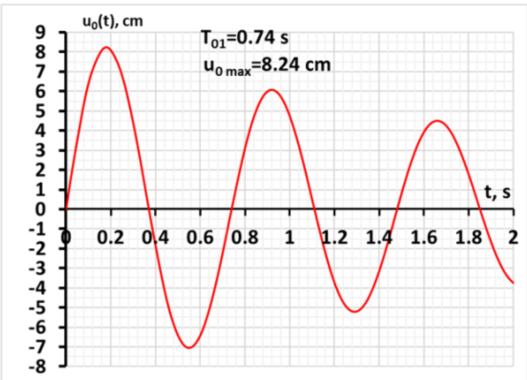
u0(t), cm
T01=0.74 s
u0 max=8.24 cm
t, s

8.

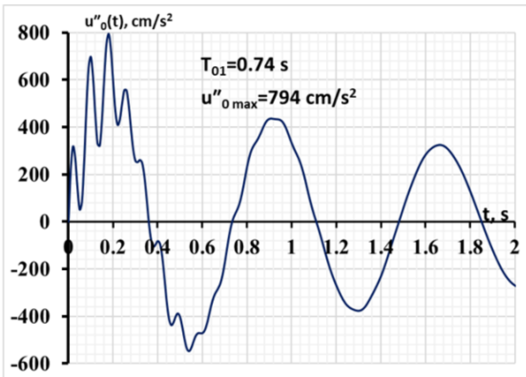
u"0(t), cm/s2
T01=0.74 s
u"0 max=794 cm/s2
t, s

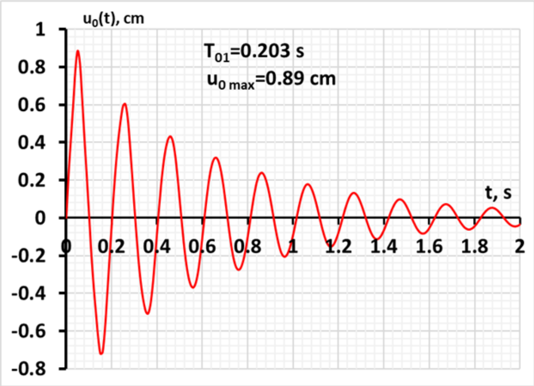
u0(t), cm
T01=0.203 s
u0 max=0.89 cm
t, s

9.

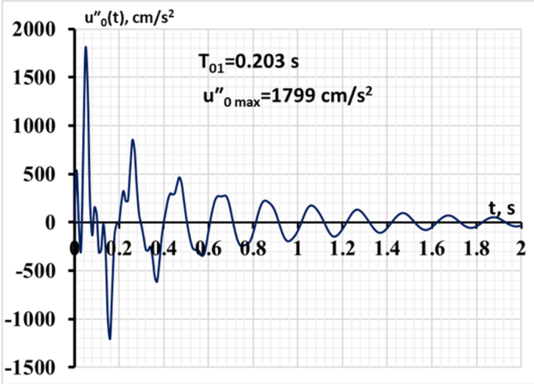
u"0(t), cm/s2
T01=0.203 s
u"0 max=1799 cm/s2
t, s

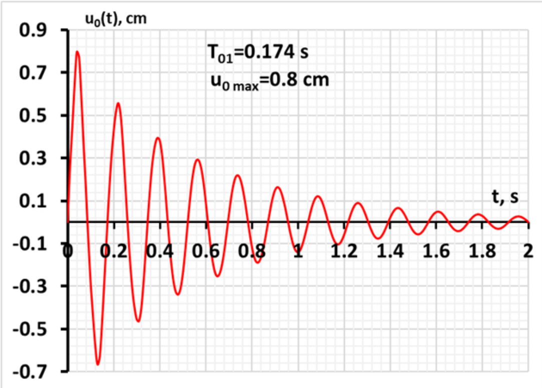
u0(t), cm
T01=0.174 s
u0 max=0.8 cm
t, s

10.

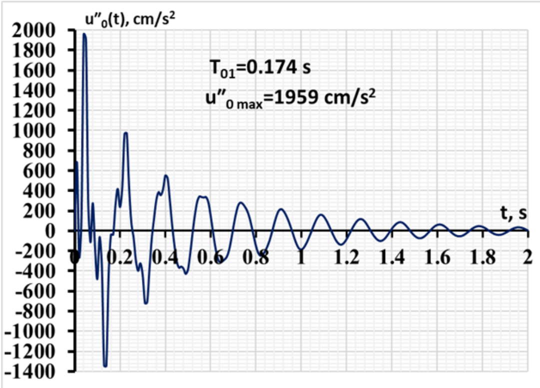
u"0(t), cm/s2
T01=0.174 s
u"0 max=1959 cm/s2
t, s

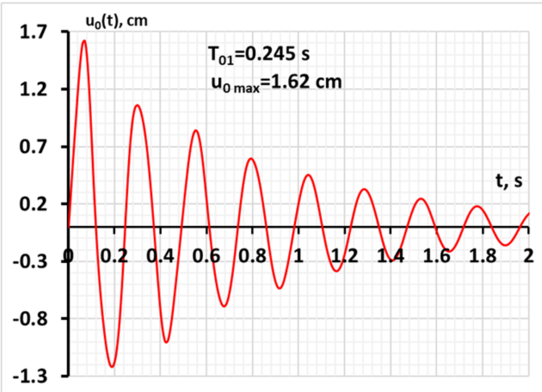
u0(t), cm
T01=0.245 s
u0 max=1.62 cm
t, s

11.

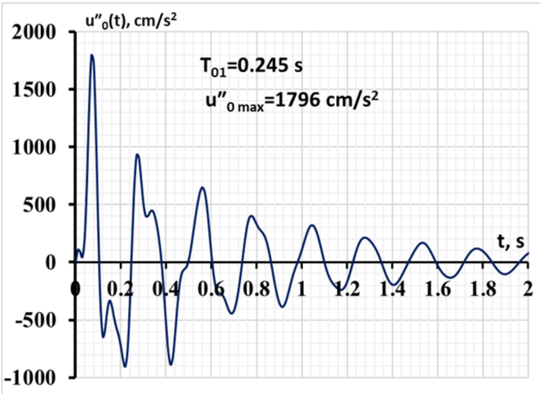
u"0(t), cm/s2
T01=0.245 s
u"0 max=1796 cm/s2
t, s

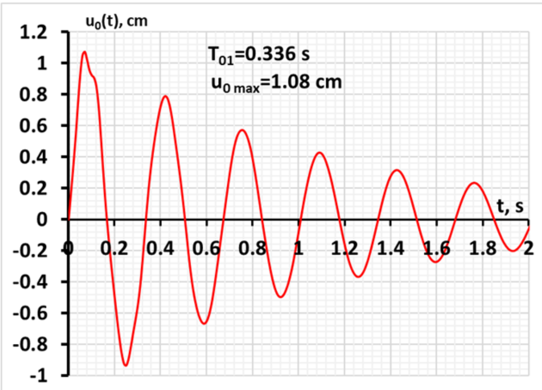
u0(t), cm
T01=0.336 s
u0 max=1.08 cm
t, s

12.

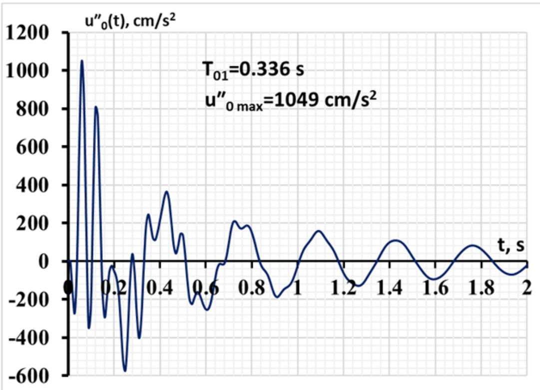
u"0(t), cm/s2
T01=0.336 s
u"0 max=1049 cm/s2
t, s

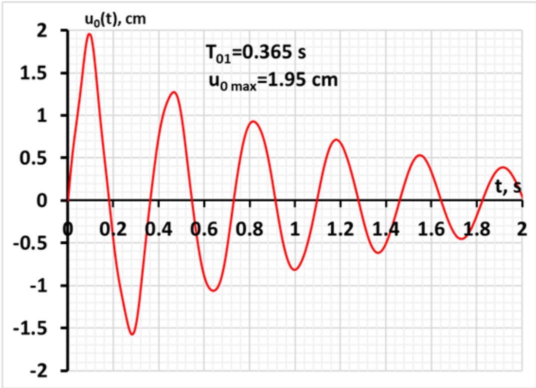

13.

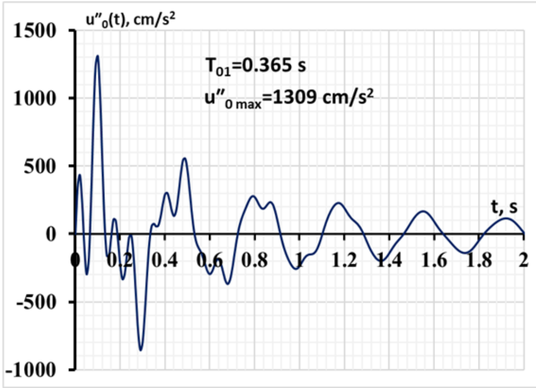

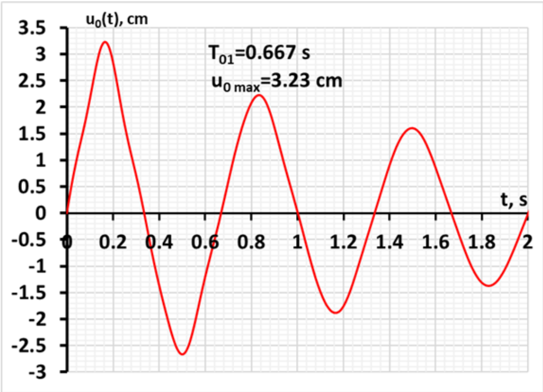

14.

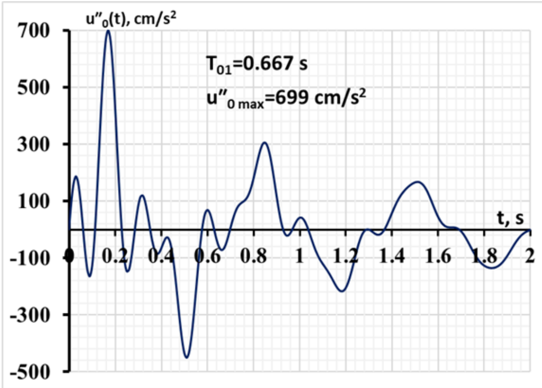

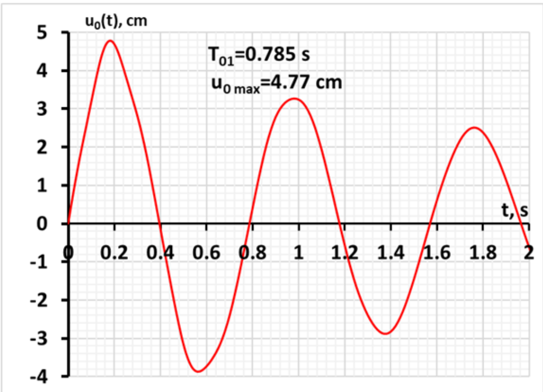

15.

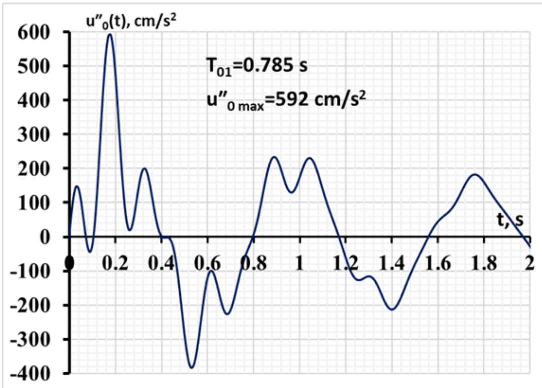

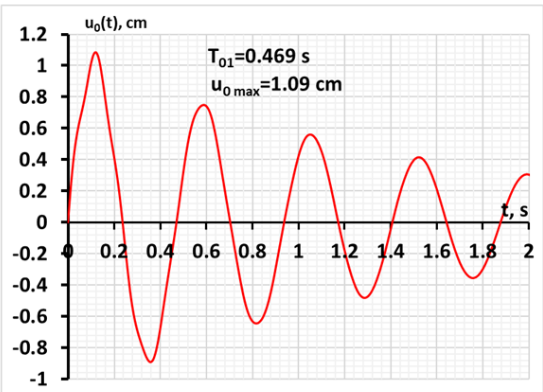

16.

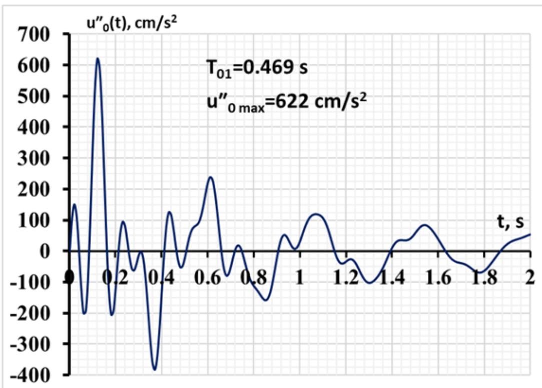

Figure 6. *Synthetic seismograms* $u_1(0,t)$ *and accelerograms* $u_1''(0,t)$ *on the surface of the earth, according to formula (25), for 16 heterogeneous bases at M=7.0,* Δ*=15 km,* $\Theta_1=\Theta_2=\Theta_3=0.3$*.*

Figure 7 presents a comprehensive overview of the dependencies of displacement and acceleration values at the ground surface on the mechanical structures of heterogeneous and homogeneous beddings, on the ratio v_{s1}/v_{s2}, and on the values of the first mode oscillation period $\overline{T}_{01}$ for heterogeneous beddings. Figure 8 supplements Figure 7 by showing how displacement and acceleration values at the ground surface vary with the increasing ratio of shear wave velocities v_{s1}/v_{s2}. As evident from Figure 7 and Table 4, for all foundations considered, the accelerations and displacements (except for the displacement value of the variant 16) calculated considering the first three oscillation modes for heterogeneous foundation beddings significantly exceed the corresponding values for equivalent homogeneous beddings.

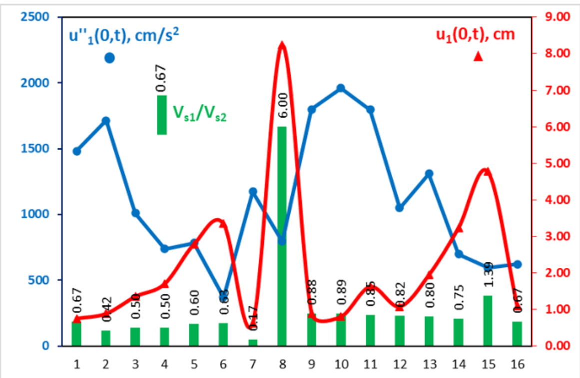

№	1	2	3	4	5	6	7	8	9	10	11	12	13	14	15	16
T_{01},s	0.207	0.232	0.380	0.458	0.657	0.925	0.246	0.740	0.203	0.174	0.245	0.336	0.365	0.667	0.785	0.469

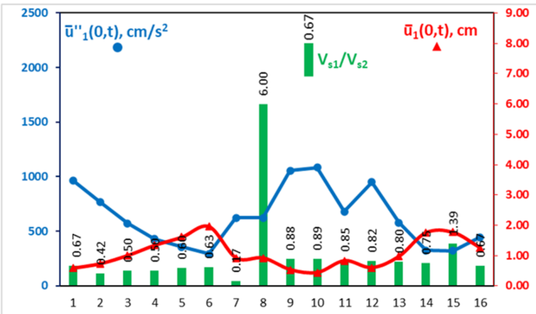

№	1	2	3	4	5	6	7	8	9	10	11	12	13	14	15	16
$\overline{T}_{01}$,s	0.233	0.293	0.400	0.533	0.640	0.780	0.367	0.367	0.211	0.182	0.332	0.241	0.390	0.700	0.705	0.505

Figure 7. *a. Peak values of accelerations $u_1''(0,t)$ (cm/s2) and displacements $u_1(0,t)$ (cm) for the 16 variants (Figure 3.) of actual two-layer heterogeneous foundation beddings, and, b. equivalent single-layer homogeneous foundation beddings, depending on the ratio v_{s1}/v_{s2}, $T_{01}, \overline{T}_{01}$ and No. of foundation (considering three oscillation modes at M=7.0, Δ=15 km, Θ1=Θ2=Θ3=0.3).*

This appears to be a very important factor distinguishing heterogeneous foundation beddings from their equivalent homogeneous counterparts.

Note that, despite the fact that the periods T_{01} for options 8 and 15 are almost the same (0.74 s and 0.78 s), the shift for option 8 is 8.24/4.77=1.73 times greater than for 15. At the same time, the data in Table 4 show that when calculating for equivalent homogeneous beddings with consideration of five oscillation modes, the average ratio of accelerations for heterogeneous and homogeneous beddings converges significantly. The data from Figures 7 and 8 indicate recurring patterns between soil displacements and accelerations: *where displacements are large, accelerations are small, and conversely, when displacements are small, accelerations are large*. This phenomenon has been repeatedly noted by Richter [15].

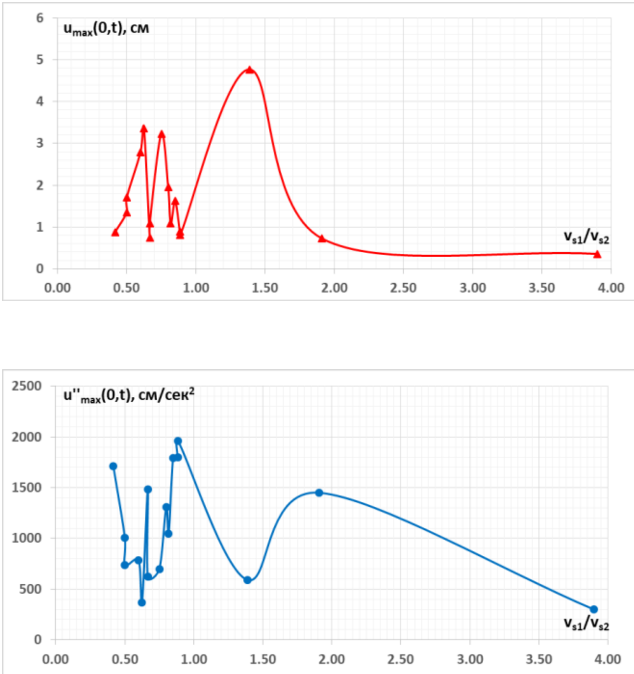

Figure 8. *Peak values of a) ground displacements $u_1(0,t)$(cm) and b) accelerations $u_1''(0,t)$ (cm/sec²) for 16 variants of beddings (excluding the heterogeneous beddings of variants No. 7 and 8 and including additional heterogeneous beddings of variants No. 17 and 18, based on Table 4) depending on the ratio v_{s1}/v_{s2}.*

In our case, for heterogeneous foundations (8), (16), ground displacements at the surface reached 8.24 cm and 4.77 cm, respectively, indicating that foundation beddings experiencing such displacements are likely unsuitable for construction, as no rock would withstand these large movements.

Using the derived formulas (25) and the δ_i, T_{0i} values presented in Tables 2 and 3, it is possible to predict not only the displacement and acceleration values at the Earth's surface (z=0) $u_{1\max}(0,t)$, $u_{1\max}''(0,t)$, but also corresponding values at any depth within the first and second layers of the heterogeneous foundation bedding. To do this, the following two equations must be applied, which are similar to formula (25):

$$0 \le z \le H_1$$
$$\begin{cases} u_1(z,t) = 100\, e^{M-8.5}\left(1-\frac{\Delta^2}{R^2}\right)\sum_{i=1}^{\infty} U_{1i}(z)\frac{T_{0i}}{2\pi}\delta_i e^{-n_i t}\sin\frac{2\pi}{T_{0i}}t \\ u_1''(z,t) = 100\, e^{M-8.5}\left(1-\frac{\Delta^2}{R^2}\right)\sum_{i=1}^{\infty} U_{1i}(z)\frac{2\pi}{T_{0i}}\delta_i e^{-n_i t}\sin\frac{2\pi}{T_{0i}}t \end{cases},$$
$$H_1 \le z \le H_1 + H_2 \quad (32)$$
$$\begin{cases} u_2(z,t) = 100\, e^{M-8.5}\left(1-\frac{\Delta^2}{R^2}\right)\sum_{i=1}^{\infty} U_{2i}(z)\frac{T_{0i}}{2\pi}\delta_i e^{-n_i t}\sin\frac{2\pi}{T_{0i}}t \\ u_2''(z,t) = 100\, e^{M-8.5}\left(1-\frac{\Delta^2}{R^2}\right)\sum_{i=1}^{\infty} U_{2i}(z)\frac{2\pi}{T_{0i}}\delta_i e^{-n_i t}\sin\frac{2\pi}{T_{0i}}t \end{cases}$$

where the values of the functions $U_{1i}(z,t)$, $U_{2i}(z,t)$ are determined by formulas (17).

According to continuity conditions (13), the displacement of the first layer $U_{1i}(z)$ at the $z = H_1$ level and the displacement $U_{2i}(z)$ of the second layer at the interface between the layers $z = H_1$ must be equal. As can be seen from (32), the quantities $u_1(z,t)$, $u_1''(z,t)$, $u_2(z,t)$, $u_2''(z,t)$, differ from each other only by the functions $U_{1i}(z)$, and $U_{2i}(z)$ in formula (17). On the ground's surface, the function $U_{1i}(z)$ at (z=0) is equal to:

$$U_{1i}(z) = \cos\frac{2\pi z}{T_{0i}v_{sl}} = 1, \quad (33)$$

Which is equal to unity for all vibration modes (i=1, 2, 3,...) and plays no role in summing the series or their final sum. On the interface between two layers, the function, $U_{2i}(z)$ after entering the values $\lambda_{1i}, \lambda_{2i}$, $z = H_1, H = H_1 + H_2$ in it, takes the form:

$$U_{2i}(z) = -\frac{\cos\frac{2\pi H_1}{T_{0i}v_{s1}}}{\sin\frac{2\pi H_2}{T_{0i}v_{s2}}}\sin\frac{2\pi}{T_{0i}v_{s2}}(H_1 - H_1 - H_2) = \cos\frac{2\pi H_1}{T_{0i}v_{s1}} \quad (34)$$

Thus, as expected, the functions $U_{1i}(z)$, $U_{2i}(z)$ coincide when $z = H_1$. However, unlike $U_{1i}(0)$, the function $U_{2i}(H_1)$ can play a role both in the values of individual terms of the series and in the final sum.

This does not occur because, as shown by the above results, the ratios of the periods of in homogeneous and heterogenuous bases are immaterial (Table 3), and the following equality holds (for homogeneous bases $T_{0i} = T_{01}/(2i-1)$):

$$\cos\frac{2\pi H_1}{T_{0i}v_{s1}} = \cos(2i-1)\frac{2\pi H_1}{T_{01}v_{s1}} = \cos\frac{2\pi H_1}{T_{01}v_{s1}}, \quad (35)$$

And therefore:

$$u_2(H_1,t) = \mu_k\, u_1(0,t), \quad u_2''(H_1,t) = \mu_k\, u_1''(0,t), \quad (36)$$

where:

$$\mu_k = \cos\frac{2\pi H_1}{T_{01}v_{s1}}. \quad (37)$$

Table 5 shows the values of the coefficients μ_k $u_{1\max}(0,t)$, $u_{1\max}''(0,t)$, calculated using the data in Table 2 (Table 4 and Figure 6), and the values $u_{2\max}(H_1)$, $u_{2\max}''(H_1)$ according to formula (36).

Table 5. *Values* $\mu_k = \cos\frac{2\pi H_1}{T_{01}v_{s1}}$ *(k-number Figure 3) of displacements and accelerations on the surface of the boundary of two layers.*

No. (Figure 3)	**Coefficient values μ_k**	**On the surface of the earth**		**At the division of two layers**	
		$u_{1\max}$, cm	**u''_{1max}, cm/sec2**	**$u_{2\max}$, cm**	**u''_{2max}, cm/sec2**
1	0.73	0.75	1482	0.54	1075
2	0.47	0.88	1714	0.41	803
3	0.68	1.35	1008	0.91	683|
4	0.61	1.7	737	1.04	449
5	0.58	2.79	782	1.61	451

No. (Figure 3)	Coefficient values μ_k	On the surface of the earth		At the division of two layers	
		$u_{1\max}$, cm	u''_{1max}, cm/sec2	$u_{2\max}$, cm	u''_{2max}, cm/sec2
6	0.69	3.35	370	2.30	253
7	0.29	0.63	1173	0.18	340
8	0.94	8.24	794	7.73	744
9	0.73	0.89	1799	0.65	1305
10	0.69	0.8	1959	0.55	1343
11	0.21	1.62	1796	0.34	381
12	0.84	1.08	1049	0.90	876
13	0.53	1.95	1309	1.03	691
14	0.59	3.23	699	1.90	411
15	0.72	4.77	592	3.43	425
16	0.95	1.09	619	1.03	587

The highest values for accelerations $u''_1(0,t)$ obtained at occurred, respectively, at ratios of $v_{s1} < v_{s2}$: 0.89, 0.88 and 0.42, 0.67, and the highest values of displacements $u_1(0,t)$ were obtained at v_{s1}/v_{s2} : 0.63, 0.75 and 1.39, 6.0.

The key finding of all mentioned studies is that when predicting seismogram and accelerogram values at the Earth's surface for heterogeneous foundation beddings, calculations using formula (25) must be performed considering no fewer than five oscillation modes, both for heterogeneous beddings and their equivalent homogeneous counterparts.

3. Conclusion

A method to predict seismograms and accelerograms for heterogeneous foundation beddings with known physical and mechanical characteristics of the bedrock layers, depending on the earthquake magnitude M≥6.0 and a given site's certain distance from the earthquake's rupture Δ (km). For 16 typical two-layer beddings in soils of various seismic categories, seismograms and accelerograms were obtained for M=7.0 and distance from rupture line Δ=15 km. A method is suggested to replace heterogeneous foundation beddings with equivalent homogeneous ones and quantitative estimates of such replacements are derived. It is shown that the fundamental oscillation mode period T_{01} of the actual heterogeneous bedding changes (both increases and decreases) by 1.05 times on average, whereas the periods of second and third oscillation mode change only slightly (by 1.01 times) compared to the periods of the second and third oscillation modes of the heterogeneous bedding. It has to be noted that with such replacements there could be an increase in ground accelerations up to 1.6 times. Calculations for the equivalent homogeneous bedding which consider five oscillation modes instead of three, show ground acceleration decreases up to 1.3 times. It has been found out that heterogeneity of the foundation bedding, in fact, leads to increased acceleration and displacement values at the ground surface due to a significant change in the natural modes of dynamic deformation of the medium (the function $U_{ki}(z)$ and coefficients δ_i) compared to the homogeneous beddings.

Abbreviations

NUACA	National University of Architecture and Construction of Armenia
NAS RA	National Academy of Sciences of the Republic of Armenia

Author Contributions

Eduard Khachiyan is the sole author. The author read and approved the final manuscript.

Conflicts of Interest

The authors declare no conflicts of interest.

References

[1] Newmark N. M. and Rosenblueth E. Fundamentals of Earthquake Engineering. Prentice-Hall, Inc. Englewood Cliffs, N.Y., 1971, 640p.

[2] Okamoto S. Introduation to Earthquake Engineering. University of Tokyo Press, 1973, 340p.

[3] Kasahara K. Earthquake Mechanics, Cambridge University Press, 1981, 264p.

[4] Brune J. N. The Physics of Earthquake Strong Motion, in Lomnitz C. and Rosenblueth E., Eds., Risk and Engineering Decisions, New York: Elsevier Sci. Publ. Co., 1976, pp. 141-177. (1976)

[5] Khachiyan E. Y., On the Possibility of Predicting Seismogram and Accelerogramof Strong Motions of the Soil for an Earthquake Model Considered as an Instantaneous Rupture of the Earth's Surface. Seismic Instruments, 2015, Vol. 51, No. 2, pp. 129-140.

[6] Khachiyan E. Y., Predicting of the Seismogram and Accelerogram of Strong Motions of the Soil for an Earthquake Model Considered as an Instantaneous Rupture of the Earth's Surface. Science Publishing Group, USA Earth Science, 2018; 7(4): 183-201, https://doi.org/10.11648/j.earth.20180704.16 (2018).

[7] Khachiyan E. Y., Analysis of the Values of Ground Displacements, Shear Strains, Velocities and Accelerations, and Response Spectra of Strong Earthquake by Synthetic Accelerograms. USA, Earth Sciences 2022; 11(5): pp. 327-337, https://doi.org/10.11648/j.eart.20221105.19

[8] RABC 20.04-2020. Earthquake Resistant Construction. Design Codes. Yerevan, 2020. 80p.

[9] Faccioli E., Resenditz D., Soil dynamics: Soil behavior under seismic actions, including liquefaction. In the book "Seismic Risk and Engineering Decisions", Elsevier Scientific Publishing Company Amsterdam-Oxford-New York 1976.

[10] E. F. Savarenskii, Seismicheskie volny (Seismic Waves), Moscow: Nedra, 1972. (in Russian)

[11] E. E. Khachiyan, Prikladnaya seismologiya (Applied Seismology), Yerevan: Gitutyun, 2008. (in Russian).

[12] E. E. Khachiyan, On Determining of the Ultimate Strain of Earth Crust Rocks by the Value of Relative Slips on the Earth Surface after a Large Earthquake. Science Publishing GroupUSA, Earth Science, https://doi.org/10.11648/j.earth.20160506.14: Vol. 5, Issue 6, Dec. 2016 pp 111-118.

[13] H. Jeffreys, and S B. Wirles, Methods of Mathematical Physics, Cambridge: Cambridge Univ., 1950, 2nd ed.

[14] Biot M. A. Analytical and Experimental Methods in Engineering Seismology. Proceedings of the American Society of Civil Engineering. 1943, 108(1), pp. 365-385, https://doi.org/10.1061/TACEAT.0005571

[15] Richter Ch. F., Elementary Seismology. W. H. Freeman and Co., San Francisco, 1958, 768p.

Biography

Eduard Khachiyan Was born 17.08.1933. Khachiyan extensive academic and research career includes roles at the Armenian Earthquake Engineering Research Institute (1956-2002), the American University of Armenia (1992-1997), and since 1997, he has served as head of the Chair of Building Mechanics at Yerevan State University of Architecture and Construction and chief scientist at the Institute of Geological Sciences of Armenia. His research focuses on applied seismology, earthquake engineering, dynamics of structures, and building mechanics. Khachiyan has authored over 290 scientific papers and received numerous accolades. His recent works include publications in Erath Sciences, Seismic Instruments and Novel Perspectives of Engineering Research. Any other remarkable point (s): Building Norms of RA II-2.02-94, II-6.02-2006, II-20.04-2020 "Earthquake engineering. Design standards" Yerevan 1994, 2006, 2020. Participation in the projects of research works primary design and re-application of the Armenian nuclear power plant.

Research Field

Eduard Khachiyan: research field 1-Applaud seismology, 2-Earthquake engineering, 3-Dynamic of Structures, 4-Building mechanics. 5-Design standards, 6-Seismic effects and Prognosis of structures behavior.

---

1 Values highlighted in green are the additional velocities of soil particles' oscillation $v\,(M, \Delta)$ for ultimate values $\Delta < R$, which are not present in the main table [7].

2 Beddings 15 and 16 (unlike the other 14 beddings) are real beddings (Gukasyan, Armenia and El Centro, USA) on which accelerograms of real earthquakes were recorded on December 7, 1988 and May 18, 1940.

3 Values of periods T_{02}, T_{03}, and $\overline{T}_{02}, \overline{T}_{03}$, are in the Table 2.

4 The ratio $\overline{\delta}_l / \overline{\delta}_i$ for any homogeneous bedding equals to $\frac{4}{\pi} \cdot \frac{(-1)^{i+1}}{2i-1}$, i=1, 2, 3…